Canadian Design Recommendations for Diagonally Reinforced Coupling Beams Using a New Comprehensive Database

Amirhossein Amiri, Tobber Lisa, and Jeremy Atkinson

Abstract Diagonally reinforced concrete coupling beams used in coupled walls are prevalent in the Canadian construction industry. In Canadian design, these beams act as seismic fuse elements that dissipate a substantial amount of earthquake energy exerted in core walls. The detailing of these beams is critical in ensuring high-energy dissipation and sufficient ductility. The Canadian Concrete handbook (CSA A23.3–14) provides engineers with guidelines to calculate the shear strength, stiffness, and ductility capacity of coupling beams. This paper presents a new comprehensive database of the hysteretic response of 51 diagonally reinforced coupled beams. With this new database, we identified trends between detailing choices and the hysteretic response and compared these trends with current Canadian codes. Specifically, the shear strength, initial stiffness, and strength loss have been examined and discussed. Overall, this study demonstrates that providing full beam confinement, as opposed to only confining the diagonal reinforcing, is a suitable method for seismic design.

Keywords Reinforced coupling beams · New comprehensive database

1 Introduction

Reinforced concrete coupled wall systems (hereafter referred to as *coupled walls*) are widely used structural systems to resist lateral loads in tall buildings. In this system, a series of concrete wall segments are connected by coupling beams to form an interconnected wall assembly. The seismic response of coupled walls depends strongly on the nonlinear behavior of the coupling beams joining adjacent wall segments.

A. Amiri · T. Lisa (✉)
School of Engineering, University of British Columbia, Kelowna, Canada
e-mail: lisa.tobber@ubc.ca

J. Atkinson
Structural Engineer with Kor Structural, Vancouver, Canada

R. Gupta et al. (eds.), *Proceedings of the Canadian Society of Civil Engineering Annual Conference 2022*, Lecture Notes in Civil Engineering 348,
https://doi.org/10.1007/978-3-031-34159-5_6

Coupling beams significantly enhance the structure's overturning resistance, stiffness, and energy dissipation compared with isolated wall piers. The construction technique used for the beam varies, but the two most common schemes utilize either diagonal reinforcing or longitudinal beam reinforcing.

Diagonal coupling beams, introduced by Paulay and Binney in 1974, are equipped with a group of diagonal bars at both the top and the bottom of the beam's section forming an "x" shape over the length of the beam. Additional longitudinal bars are provided in the corners and sides of the beams to anchor ties and provide crack control. Based on previous experimental programs, the application of diagonal layouts in coupling beams instead of conventional longitudinal reinforcing has led to higher energy dissipation and ductility.

Several experimental programs regarding diagonally reinforced coupling beams (DRCBs) with different test setups were conducted previously each of which included a number of specimens with different geometry, reinforcement arrangement, and detailing. Additionally, some databases about DRCBs have been collected concentrating on specific design parameters, i.e., [14] collected a comprehensive database regarding the initial stiffness of diagonally reinforced coupling beams. However, these databases either did not include an adequate number of studied specimens (for instance [20] or they focused only on a specific designing parameter. In this study, an up-to-date and comprehensive database is collected to derive empirical equations for designing purposes based on Canadian design provisions and instructions.

In this paper, the Canadian detailing and design equations for coupling beams are compared with experimental data from a newly developed database of 51 diagonally coupling beams which is presented in Sect. 3. This analysis provides insights into the coupling beam shear strength, stiffness, and ductility, which are presented in Sect. 4.

2 Design Provisions for Diagonally Reinforced Coupling Beams

2.1 CSA A23.3 Design Provisions

In Canada, coupled walls are designed and detailed according to the CSA A23.3–19 and the National Building Code (NBC) [23]. Figure 1 shows a typical layout for diagonally reinforced coupling beams in Canada and some of the geometric limitations of the design. According to the CSA A23.3, the width (b_w) and height (h) of the coupling beam should not exceed the pier wall's thickness (t_w) and two times the clear length of the coupling beam (L), respectively. It is required that each group of diagonal bars includes at least four bars. Moreover, CSA A23.3–19 requires that the minimum embedment length of diagonal bars into the pier walls at each end should be at least 1.5 L_d, where L_d is the development length of bars.

The design force and deformation demand in coupled wall systems are typically determined using the linear dynamic method in the NBC. As the coupling beams

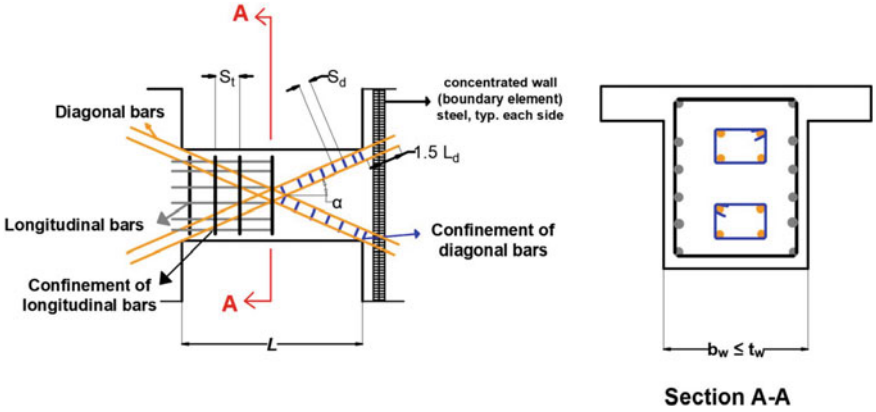

Fig. 1 General CSA A23.3 provisions for diagonally reinforced coupling beams

deform in an earthquake, they will crack, and their stiffness will degrade. For the purpose of linear dynamic analysis, an effective cracked section stiffness is accounted for by applying stiffness modification factors to the finite elements used to model the beams. The effective shear area and the effective moment of inertia are shown in Eqs. 1 and 2, respectively.

$$A_{\text{ve}} = \alpha_s A_g \tag{1}$$

$$I_{\text{eff}} = \alpha_f I_g \tag{2}$$

where A_g is the beam's gross area, and I_g is the beam's gross moment of inertia. The CSA A23.3–19 recommends modifying coupling beams' shear area and moment of inertia by using $\alpha_s = 0.45$ and $\alpha_f = 0.25$, respectively.

$$V_n = 2A_{S,d} \times f_{y,d} \times \sin\alpha \tag{3}$$

where $A_{S,d}$ is the total area of the diagonal bars at the top or bottom of the beam's section, $f_{y,d}$ is the yielding strength of diagonal bars, and α is the inclination angle between the diagonal bars and the beam longitudinal axis.

To prevent the diagonal bars from buckling, the bundles of diagonal bars are required to be tied by crossties and hoops. The spacing of these diagonal ties is determined using Eq. 4 based on CSA A23.3–14 clause 21.5.8.2.4.

$$S_d \leq \min\{6d_b, 24d_{\text{tie}}, 100\text{mm}\} \tag{4}$$

where S_d is the diagonal tie spacing, d_b is the diagonal bars' diameter (mm), and d_{tie} is the hoops or crossties' diameter (mm).

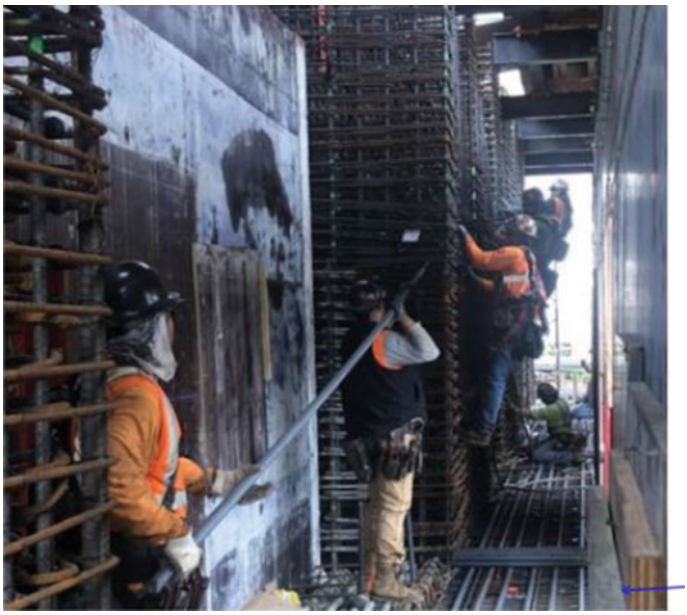

Fig. 2 Crew of five insert #11 (35 M) diagonal bars through wall boundary elements and into a diagonal coupling beam

For most typical applications in tall buildings, beams will use 10 M ties and 20 M or larger diagonal bars, so the 100 mm spacing governs.

It is worth noting that in American codes [21], (i.e., ACI 318–19) designers have the option of either providing confinement around the diagonals or confining the entire beam cross section. However, there are currently no clauses within the CSA A23.3–19 that allow such a design [22]. Confining the entire beam cross section was introduced in ACI 318–08 in light of the results from [14]. This option is often preferred by fabricators because it can simplify the installation of diagonal reinforcing, which is a considerable challenge in heavily reinforced walls (see Fig. 2).

2.2 ACI 318–19 Design Provisions

The ACI requirements for full beam confinement (clause 18.10.7.4d) include minimum reinforcing ratio related to beam geometry and materials (Eq. 5), and maximum spacing between tie legs (S_t) in all three spatial directions (Eq. 6). Spacing between tie legs perpendicular to the longitudinal axis must be less than 200 mm and engage a longitudinal peripheral bar. The peripheral bars are not intended to embed into the adjacent wall piers.

Table 1 ACI 318–19 includes requirements for coupling beams with diagonal confinement

Diagonal requirements	
Diagonal bar group width	$\geq \frac{b_w}{2}$
Diagonal bar group height	$\geq \frac{b_w}{5}$
Total cross-sectional area of transverse reinforcement within the spacings	$A_{\text{sh}} \geq \max\left\{0.09 s_t b_c \frac{f'_c}{f_{\text{yt}}}, 0.3 s_t b_c \left(\frac{A_g}{A_{\text{ch}}} - 1\right) \frac{f'_c}{f_{\text{yt}}}\right\}$
Beam requirements	
Beam tie spacing	$S_t \leq \min\left\{\frac{A_v}{0.002 b_w}, 300\,\text{mm}\right\}$
Longitudinal reinforcement	$A_{s,\text{long}} \geq 0.002 b_w s \& s \leq 300\,\text{mm}$

*where A_v is the area of transverse reinforcement; $A_{s,\text{long}}$ is the peripheral longitudinal reinforcement total area, and s is the spacing between longitudinal bars.

$$\rho = \frac{A_{\text{sh}}}{s_t \times b_c} \geq \max\left\{0.09 \frac{f'_c}{f_{yt}}, 0.3\left(\frac{A_g}{A_{\text{ch}}} - 1\right) \frac{f'_c}{f_{yt}}\right\} \tag{5}$$

where ρ is the minimum reinforcing ratio, b_c is the confined beam width, A_{sh} is the total cross-sectional area of transverse reinforcement (including crossties) within spacing S_t and perpendicular to b_c; A_g is the overall beam cross-section area; A_{ch} is the confined beam cross-section area, and f_{yt} is the yield strength of the transverse bars.

$$S_t \leq \min\{150\text{mm}, 6d_b\} \tag{6}$$

It is also interesting to note that for beams with diagonal confinement, ACI 318–19 includes requirements on the size of the diagonal group of bars, minimum number of confining ties, and minimum beam reinforcing in clause 18.10.7.4c. A minimum area of ties around the diagonal often results in significantly more ties than A23.3 would require. These requirements provide more explicit detailing constraints than A23.3 and are summarized below (Table 1).

3 Specimen Database

The experimental data from 51 diagonal coupling beam specimens were collected and a database was developed. The studied specimens were tested between 1974 and 2020. Each specimen underwent cyclic loading until failure was observed, or underwent cyclic loading then was loaded monotonically until failure (like Paulay et al., 1974 and Adebar et al., 2001). Various factors were considered in selecting each specimen, including aspect ratio (L/h); axial restraint (AR); embedment of longitudinal bars (ELB); and diagonal ties.

Aspect ratio (L/h) is considered an essential factor in coupling beams design. The database considers specimens with aspect ratios between 1 and 5, as shown in Fig. 3a. Based on the experimental testing, coupling beams with a low aspect ratio, (i.e., $L/h < 2$) behave like stocky beams with high shear deformation and a dominant shear failure mode. On the other hand, coupling beams with higher aspect ratios, (i.e., $L/h >= 2$) act like slender beams, where higher flexural deformation and more flexural yielding are observed.

The embedment of longitudinal bars (ELB) into the pier walls in coupling beams is not recommended by Canadian design codes. However, numerous experiments were completed where the longitudinal reinforcing extended significantly into the wall. The embedment allows for this longitudinal reinforcing to develop strength and, therefore, affects the cyclic response. Figure 3b shows the number of specimens within the database with this embedded longitudinal reinforcing.

Axial restraint (AR) refers to tests that attempt to restrain the coupling beam from any longitudinal movement. In this study, the inclusion of slabs is considered an axial restraint, as slabs were included in numerous experiments, (i.e., [14], Ishikawa et al. 1996 [3]). In some studied experimental programs, the researchers used prestressed or posttensioned bars to create axial forces prior to loading the specimens, acting like axial restraints ([6], [14], Brian [17]). Another method of axial restraint considered

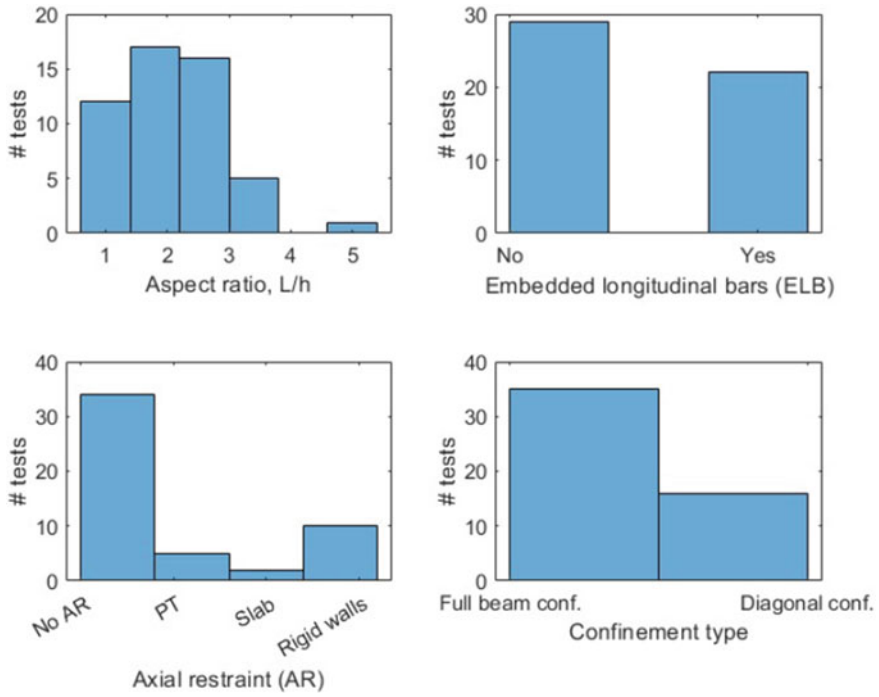

Fig. 3 Characteristics of coupling beams in the database

in the database, and the most rigid, is by preventing the testing setup from axial movement (Kwan et al., 2002, [12, 13], Han et al. [19]). Figure 3c shows the different types of axial constraints within the database.

The majority of tests utilized "beam confinement," where ties are only provided in the beam, and no ties are provided along the diagonal rebars. While the Canadian code does not provide guidance for this type of detail, the data from these tests are included in this analysis. Figure 3d shows the number of tests for each type of confinement.

Table 2 summarizes the authors, specimen names, geometry, materials, and reinforcement details. In these Tables, S_d and S_t are the spacing of the diagonal ties and the beam ties, respectively.

4 Analysis of the Normalized Experimental Data

To systemically study all of the data in the database, each critical parameter was normalized to important Canadian design parameter. In this regard, the backbone parameters shown in Fig. 4 were examined and compared with assumptions used in Canadian design. Specifically, we looked at the initial stiffness (K_i), the maximum shear strength (V_{max}), and the rotation corresponding to the shear strength of 0.8Vmax ($\theta_{80\%}$).

Inelastic rotational capacity is one of the most important factors in the seismic design of reinforced concrete elements. It represents the ability of the element to deform while maintaining strength. In this study, the degradation rotation ($\theta_{80\%}$) is taken as the rotation when the force on the experimental backbone degrades to 80% of the peak shear force. This parameter was used as an indicator of the inelastic rotational capacity. Further loading beyond this point would exhibit a significantly degraded shear capacity, and the beams would be in a severely damaged state.

The following sections compare the experimental response of each specimen with Canadian design practice. In this study, the backbone in both the positive and negative directions was assessed, and the maximum absolute values were selected in the analysis.

4.1 Maximum Shear and Overstrength

The maximum observed shear force and overstrength of coupling beams are important for capacity design and nonlinear modeling. Overstrength was determined as the ratio between the maximum observed shear force (V_{max}) and the nominal shear force (V_{ne}) calculated per Eq. 3 using reported material strength. Figure 5 shows the range of calculated overstrength for all specimens, axial restraint (AR), embedded longitudinal bars (ELB), both AR and ELB, and neither AR nor ELB.

Table 2 Specimens database

	Author	Name	L/h	ELB	AR	Sd mm	St mm	α °	b_w mm	h mm	f'c Mpa	Diagonals		
												#	Name	fy, Mpa
L/h < 2	[1]	Beam 316	1.29	No	None	None	150	36	152	787	33	4	#7	288
												3	#8	287
		Beam 317	1.29	No	None	100	150	36	152	787	51	4	#7	306
												3	#8	270
		Beam 395	1.03	No	None	100	150	20	152	991	36	4	#7	259
												3	#8	289
	Ishikawa and Kimura [3]	1	1.78	Yes	None	None	90	17.5	300	450	42	4	D22	523
		2	1.78	Yes	None	None	90	17.5	300	450	46	6	D22	523
		3	1.78	Yes	None	None	90	17.5	300	450	45	6	D22	523
		4	1.78	Yes	Slab	None	90	17.5	300	450	48	6	D22	523
		5	1.78	Yes	None	None	45	17.5	300	450	27	6	D22	523
		6	1.78	Yes	None	None	25	17.5	300	450	51	6	D22	523
		7	1.78	Yes	None	None	90	17.5	300	450	52	6	D22	523
		8	1.78	Yes	None	None	90	17.6	300	450	45	8	D19	387
	[5]	P07	1.5	Yes	Rigid	None	120	28.5	150	400	54	8	#3	566
		P12	1.5	Yes	Rigid	150	120	28.5	150	400	42	8	#3	566
	[7]	D30	1.136	No	None	60	275	30	300	880	33	8	20-M	456
	[8]	CCB11	1.17	Yes	None	60	140	35.8	120	600	37.8*	12	T8	517
	[11]	S1	1	Yes	None	75	75	36	200	600	41	8	D13	450
	[12]	CB-1	1	Yes	Rigid	None	150	30	200	600	44	4	D16	474

(continued)

Table 2 (continued)

	Author	Name	L/h	ELB	AR	Sd mm	St mm	α °	b_w mm	h mm	f'c Mpa	Diagonals		
												#	Name	fy, Mpa
	[15]	CB10-1	1	Yes	None	None	100	26	250	500	35	8	D25	486
	[17]	CC-16d_b	1.136	No	None	320	300	30	300	880	38	8	20 M	457
		MD-10d_b	1.136	No	None	200	300	30	300	880	42	8	20 M	457
		MD-8d_b	1.136	No	None	160	300	30	300	880	43	8	20 M	457
		D-6d_b	1.136	No	PT	120	300	30	300	880	45	8	20 M	457
	[18]	CB1A	1.89	No	PT	None	76.2	18	250	460	44	12	#7	434
	[20]	CB1	1.89	No	None	None	76.2	18	254	457	41	12	#7	434
L/h > 2	[2]	C6	2.5	No	None	None	33.8	19	102	169	18.1	1	#4	408
		C8	5	No	None	None	33.8	9.5	102	169	23.9	1	#4	433
	[4]	LX7L	2.8	Yes	None	None	80	12.9	240	350	37.7	8	D16	528
		NX7L	2.8	Yes	None	None	80	12.9	240	350	38.1	8	D16	528
	[6]	K1	2.74	No	PT	100	244	12.3	305	445	35.6	8	30-M	464
	[9]	CB-2	3	Yes	None	None	110	14.6	300	500	35.6	4	25 M	461
	[10]	N-1	2.5	Yes	None	None	150	19.3	200	400	54	8	D16	476
		N-2	2.5	Yes	None	None	100	19.3	200	400	51	8	D16	459
	[13]	DCB1	2.57	Yes	None	76	76	13	254	356	37.6	4	#8	431
		DCB2	3	No	None	51	51	13	254	305	55.3	4	#7	477
	[14]	CB24F	2.4	No	None	None	76	15.7	305	381	47.2	12	#7	482

(continued)

Table 2 (continued)

	Author	Name	L/h	ELB	AR	Sd mm	St mm	α °	b_w mm	h mm	f'c Mpa	Diagonals		
												#	Name	fy, Mpa
		CB24D	2.4	No	None	63.5	63.5	15.7	305	381	47.2	12	#7	482
		CB24F-RC	2.4	No	Slab	None	76	15.7	305	381	50.4	12	#7	482
		CB24F-PT	2.4	No	PT	None	76	15.7	305	381	49.9	12	#7	482
		CB24F-1/2-PT	2.4	No	PT	None	152.4	15.7	305	381	48.2	12	#7	482
		CB33F	3.33	No	None	None	76	12.3	305	457	47.2	12	#7	482
		CB33D	3.33	No	None	63.5	63.5	12.3	305	457	47.2	12	#7	482
	[15]	CB20-1	2	Yes	None	None	100	16	300	500	52.1	8	D29	466
	[16]	CB30DA	3	Yes	None	150	200	8.8	300	500	39.7	8	#10	464
		CB30DB	3	Yes	None	None	100	8.8	300	500	38.4	8	#10	464
	Whan [19]	T1002.0	2	No	Rigid	None	120	20.4	250	525	44	8	D22	477
		T772.0	2	No	Rigid	None	170	20.4	250	525	43	8	D22	477
		T502.0	2	No	Rigid	None	250	20.4	250	525	43	8	D22	477
		T302.0	2	No	Rigid	None	300	20.4	250	525	43	8	D25	481
		T1003.5	3.5	No	Rigid	None	110	8.9	250	300	43	8	D25	481
		T50-3.5	3.5	No	Rigid	None	250	8.9	250	300	44	8	D25	481
		T30-3.5	3.5	No	Rigid	None	500	8.9	250	300	44	8	D25	481

* Value is calculated cylinder strength based on cube test

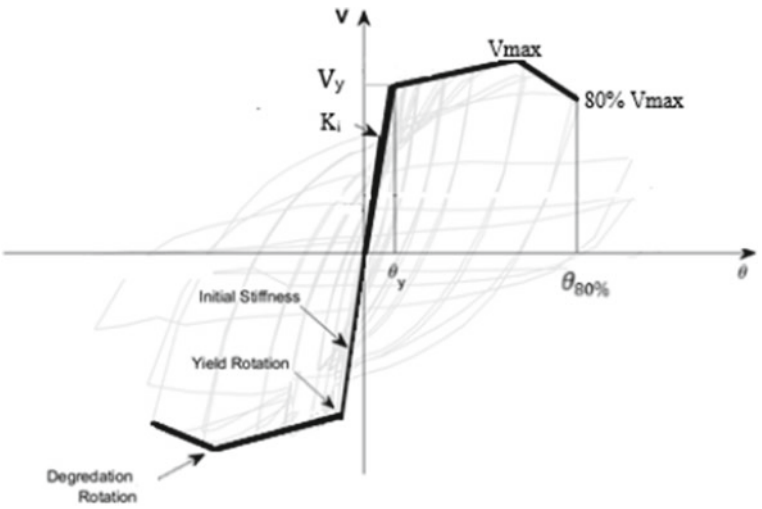

Fig. 4 Backbone curve for coupling beam models

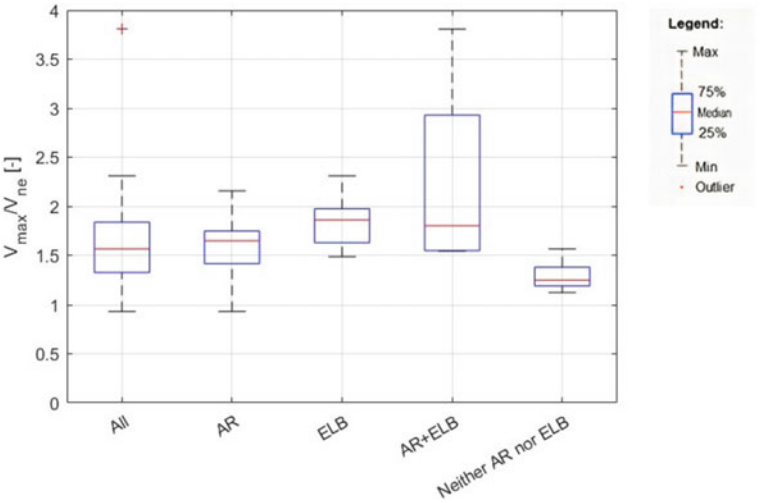

Fig. 5 Range of overstrength for specimens with different characteristics: (i) All specimens, (ii) Axial restrained (AR), (iii) Embedded longitudinal bars (ELB), (iv) Both AR and ELB, and (v) Neither AR nor ELB

The median overstrength for all specimens was approximately 1.55. AR or ELBs contribute to higher median overstrength, ranging from 1.6 for AR only (13 specimens) to 1.8 for ELB only (19 specimens). For the four specimens with AR and ELB, the median overstrength was 1.7, but the variability was large. For example, some specimens had an overstrength exceeding 3.0. When neither AR nor ELB was

present (15 specimens), the median overstrength was approximately 1.25. In short, both AR and ELB are observed to increase the overstrength.

4.2 Effect of Embedded Longitudinal Bars

In order to investigate the effect of embedded longitudinal bars in the shear strength of specimens, a new term of shear strength named "V_t" is introduced. Based on Eq. 7, V_t equals the summation of nominal shear force calculated per Eq. 3 and the shear force corresponding to the flexural resistance (V_{me}), calculated per Eq. 8. To obtain V_{me}, it is required to calculate the nominal moment capacity (M_n). Flexural capacity of coupling beams (M_n) is obtained by using Eq. 9.

$$V_t = V_{me} + V_{ne} \tag{7}$$

$$V_{me} = \frac{2M_n}{L} \tag{8}$$

$$M_n = A_{\text{sl}} f_{\text{yl}}\left(d - d'\right) \tag{9}$$

where A_{sl} is the total area of longitudinal bars, f_{yl} is the yield strength of longitudinal bars, and d and d' are the effective depths of longitudinal bars in tension and compression zones, respectively.

Figure 6 illustrates the effect of embedded longitudinal bars on the shear strength of specimens. In this figure, the ratio of $V_{\max}$ over V_t is shown in the vertical axis. Different types of specimens in terms of mechanical features were described in the horizontal axis.

As was expected, the median overstrength of specimens without axial restraint and without embedded longitudinal bars is the same as the one plotted in Fig. 5. On the other hand, the median overstrength is equal to 1.25 and 1.3 for ELB and AR + ELB, respectively. Hence, V_t is a reasonable method of estimating the shear force of coupling beams which have embedded longitudinal reinforcing.

4.3 Effect of Axial Restraint

The presence of axial restraint impacts the behavior of coupling beams significantly. Generally, axial restraints would result in higher strength and lower elongation of coupling beams. In this regard, Fig. 7 shows the overstrength of specimens equipped with no axial restraint, and different types of axial restraints, namely prestressed rods (PT), slab, and rigid walls.

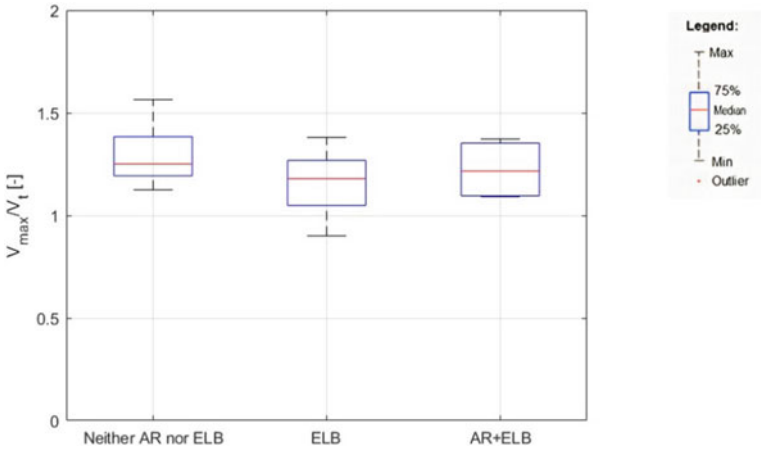

Fig. 6 Range of overstrength including the impact of embedded longitudinal bars for specimens with different characteristics: (i) All specimens, (ii) Axial restrained (AR), (iii) Embedded longitudinal bars (ELB), (iv) Both AR and ELB, and v) Neither AR nor ELB

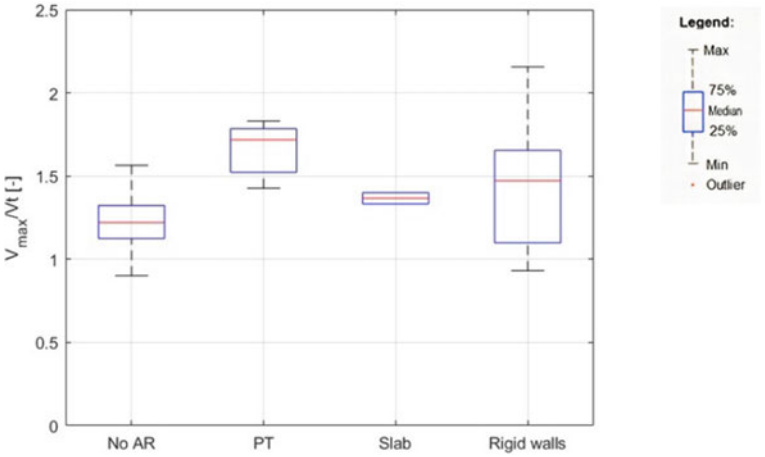

Fig. 7 Range of overstrength including the impact of embedded longitudinal bars for specimens with different types of axial restraint: (i) No axial restraint, (ii) Prestressed rod, (iii) Slab, iv) Rigid walls

According to Fig. 7, specimens without any axial restraints have median overstrength of 1.25. The median overstrength in specimens with slabs is equal to 1.4. This additional overstrength is attributed to the larger compression block provided by the slab. Specimens restrained in the axial direction with PT rods had a median overstrength of about 1.75. This PT overstrength is due to the additional compression load induced by the PT which the calculation of V_t does not account for. Finally,

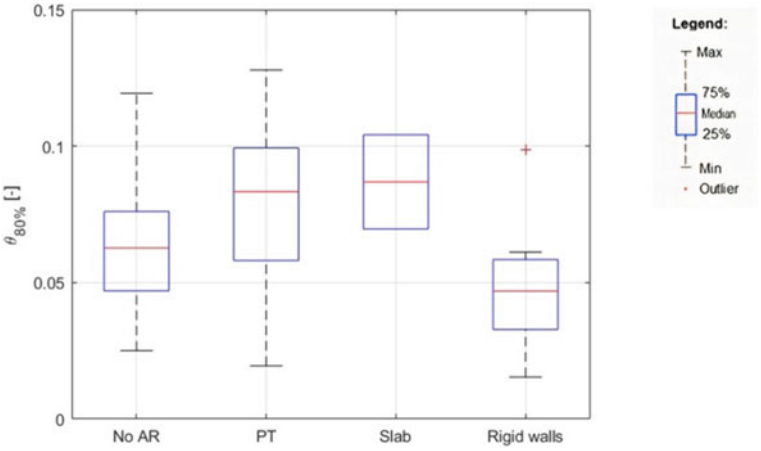

Fig. 8 Range of degradation rotation ($\theta_{80\%}$), for specimens with different types of axial restraint: i) No axial restraint, ii) Prestressed rods, iii) Slab, iv) Rigid walls

the overstrength provided by rigid walls is approximately 1.5. The cause of this overstrength is likely due to contributions from the experimental setup.

Figure 8 depicts the value of degradation rotation ($\theta_{80\%}$) for specimens with different types of axial restraint. According to this figure, the median $\theta_{80\%}$ for specimens with PT rods and slabs is almost 8%, exceeding the median $\theta_{80\%}$ of specimens without axial restraint by about 30%. In the case of the PT, this additional ductility is likely provided by the PT closing cracks and restricting excessive elongation. Similarly, the slab specimens provide added resistance to degradations.

Specimens with rigid axial restraint has the lowest amount of median $\theta_{80\%}$ which is equal to 4.9%. It is anticipated that the rigid restraint provided by the test setup does not permit the cracks to close effectively, resulting in early strength loss.

4.4 Effect of Diagonal Tie Spacing on $\theta_{80\%}$

Figure 9a, b shows $\theta_{80\%}$ of beams with diagonal ties compared with the ratio of diagonal tie spacing (S_d) to the spacing calculated according to the CSA A23.3 (Eq. 4) for L/h < 2 and L/h ≥ 2, respectively. Figure 9 also exhibits the ductility capacity provided by CSA A23.3, which is 0.04 radians (red line). CSA A23.3 requires designers to consider the minimum inelastic ductility demand of coupling beams equal to this value through their design procedures.

Overall, Fig. 9 depicts that there is little correlation between diagonal tie spacing and ductility. A number of specimens with L/h < 2 exhibited ductility's which are lower than the CSA A23.3 limit, even those where the S_d was less than the $S_{d,\,CSA}$.

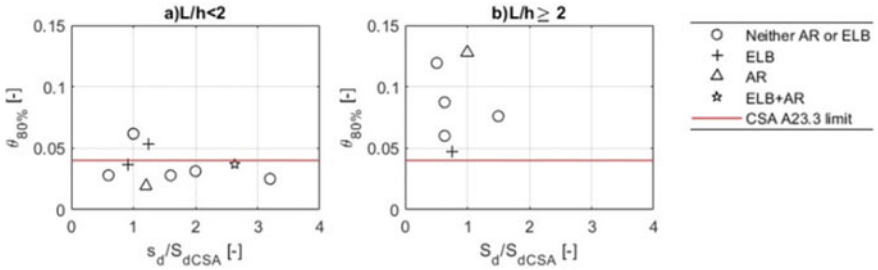

Fig. 9 Degradation rotation ($\theta_{80\%}$) versus diagonal tie spacing for specimens with **a** L/h < 2 and **b** L/h ≥ 2

On the other hand, all specimens are shown in Fig. 9b with L/h ≥ 2 and diagonal ties result in high $\theta_{80\%}$, satisfying the CSA A23.3–19 minimum acceptable value.

4.5 Effect of Beam Tie Spacing on $\theta_{80\%}$

Figure 10a, c show $\theta_{80\%}$ of beams with full confinement compared with the ratio of beam tie spacing (S_t) to half of the beam depth (h/2) for L/h < 2 and L/h ≥ 2, respectively. Figure 10b, d illustrate of beams with diagonal confinement compared with the ratio of beam tie spacing (S_t) to half of the beam depth (h/2) for L/h < 2 and L/h ≥ 2, respectively. For reference, the minimum ductility capacity provided by CSA A23.3, which is 0.04 radians is shown in Fig. 10.

According to Figs. 10a, c, it can be observed that decreasing the beam tie spacing, (i.e., increasing the confinement of the overall beam) increases $\theta_{80\%}$. Furthermore, it is visible that most of the specimens with full beam confinement layouts have an amount of $\theta_{80\%}$ between 0.04 and 0.1.

Figure 10b shows that for specimens with L/h < 2, increasing the beam tie spacing in beams that have diagonal ties results in a decrease of $\theta_{80\%}$. This result implies that beam tie spacing is also a critical variable in the ductility capacity of diagonally reinforced coupling beams, and guidance should be provided to designers.

4.6 Effect of the Transverse Reinforcement Ratio (ρ_V)

Transverse reinforcement ratio (ρ_v), which is calculated by Eq. 10, is recognized as an important design factor.

$$\rho_v = \frac{A_v}{b_w s_t} \tag{10}$$

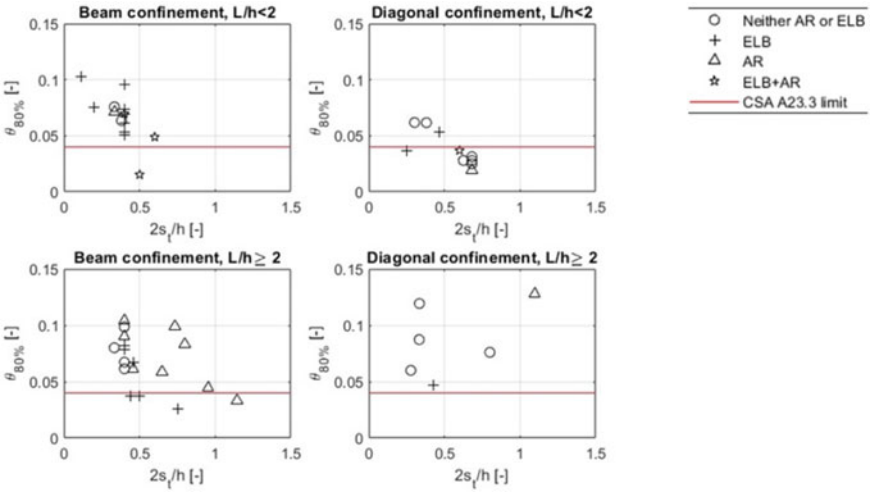

Fig. 10 Degradation rotation ($\theta_{80\%}$) versus beam tie spacing for specimens with **a** Beam conf. layout and L/h < 2, **b** Diagonal conf. and L/h < 2, **c** Beam conf. layout and L/h ≥ 2, **d** Diagonal conf. and L/h ≥ 2

Figure 11a, c show $\theta_{80\%}$ of beams with full beam confinement compared with ρ_v for L/h < 2 and L/h ≥ 2, respectively. Figure 11b, d illustrates $\theta_{80\%}$ of beams with diagonal confinement compared with ρ_v for L/h < 2 and L/h > = 2, respectively.

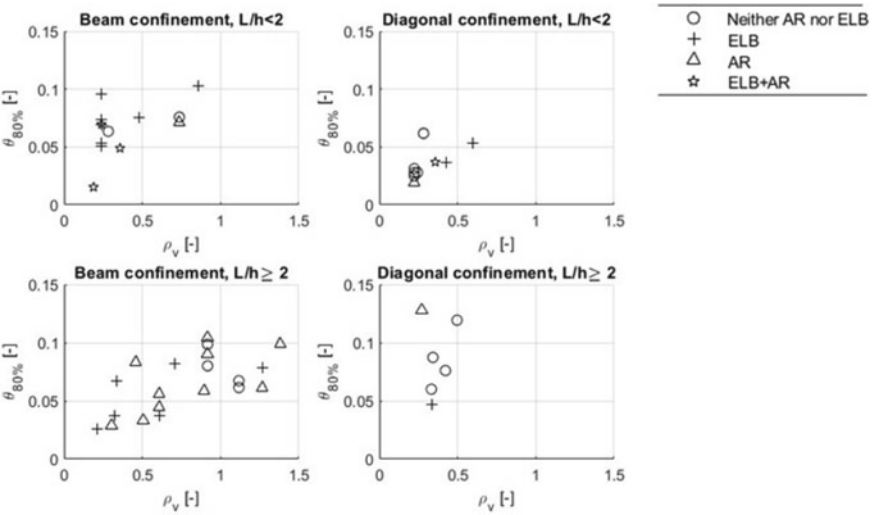

Fig. 11 Degradation rotation ($\theta_{80\%}$) versus beam tie spacing ratio for specimens with **a** Beam conf. layout and L/h < 2, **b** Diagonal conf. and L/h < 2, **c** Beam conf. layout and L/h ≥ 2, **d** Diagonal conf. and L/h ≥ 2

Based on Figs. 11a, c, it could be concluded that the more amount of transverse reinforcement ratio in the coupling beams with full beam confinement layout would result in more $\theta_{80\%}$. However, according to Figs. 11b, d, it seems that the amount of transverse reinforcmenet ratio does not impact the degradation rotation of the coupling beams with diagonal confinement layout.

4.7 Initial Stiffness (K_i)

The initial stiffness of the coupling beam (K_i) is important when utilizing the dynamic analysis to determine seismic demands on the structure. It is also a critical parameter in determining structural period and developing appropriate models for performance-based design.

The initial stiffness of a coupling beam can be determined by summing the flexural deformation (Δ_F) and shear deformation (Δ_S). The total displacement of a coupling beam (Δ_T) is calculated using Eq. 11.

$$\Delta_T = \frac{V_y}{K_i} = \Delta_F + \Delta_S \tag{11}$$

where V_y is the applied shear force; K_i is the initial stiffness; Δ_F is the flexural deformation (shown in Eq. 12), and Δ_S is the shear deformation (shown in Eq. 13).

$$\Delta_F = \frac{V \times L^3}{E_c \times I_{\text{eff}}} \tag{12}$$

$$\Delta_S = \frac{V \times L}{G_c \times A_{\text{ve}}} \tag{13}$$

where I_{eff} is the effective moment of inertia (Eq. 2), A_{ve} is the effective shear area (Eq. 1); E_c is the elastic modulus of reinforced concrete $\left(E_c = \left(3300\sqrt{f_c'} + 6900\right)\left(\frac{\gamma_c}{2300}\right)^{1.5}\right)$; f_c' is the compression strength of concrete; γ_c is the concrete density factor which is equal to 2300 kg/m^3 in this study; G_c is the shear modulus of reinforced concrete; $G_c = \frac{E_c}{2(1+\nu)}$, and ν is Poisson ratio which has been chosen to 0.25 in this study.

By substituting Eqs. 12 and 13 into Eq. 11 the initial stiffness of the coupling beam is determined and presented in Eq. 14.

$$K_i = b_w \times E_c \times C_K \tag{14}$$

where C_k is a unitless parameter shown in Eq. 15.

$$C_K = \frac{\alpha_f.\alpha_s}{2(1+\nu).\alpha_f.\left(\frac{L}{h}\right) + \alpha_s.\left(\frac{L}{h}\right)^3} \tag{15}$$

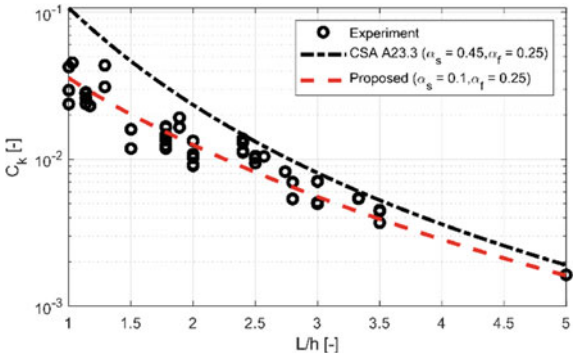

Fig. 12 C_K values based on various amounts of α_f and α_s

Using the unitless parameter C_K, the experimental results were compared with the effective cracking parameters used by the CSA A23.3–19. In this comparison, the experimental C_K values were determined using Eq. 16.

$$C_K = \frac{K_i, \exp}{b_w E_c} \tag{16}$$

where $K_{i,\exp}$ is the initial stiffness obtained from experiment's results.

Figure 12 shows the effective stiffness parameters $\alpha_s = 0.45$ and $\alpha_f = 0.25$ recommended by CSA A23.3–19, the experimental values, and a new recommendation value of $\alpha_s = 0.1$ and $\alpha_f = 0.25$.

Based on the results shown in Fig. 12, the code equation appears to be an upper bound of the stiffness of coupling beams. However, the proposed values exhibit almost comprehensive coverage over the stiffness of coupling beams.

5 Conclusions

The behavior of diagonally reinforced coupling beams is a critical factor in the seismic performance of coupled wall systems, commonly used in seismically active areas worldwide. The coupling beam elements provide significant energy dissipation over the structure's height and induce large forces into the wall piers. With the increasing use of nonlinear time-history analysis as an assessment and design tool, accurate understanding of structural elements is an important research effort. The discussions in this paper, as well as the empirical relations, can help inform engineers in both performances-based design and assessment.

Some of the key conclusions from this paper are:

- Axial restraint and embedded longitudinal bars can considerably increase the overstrength of the coupling beam. The median amount of overstrength varied from 1.6 for axially restrained, 1.8 for embedded longitudinal bars, and 1.7 for

beams with both axially restraint beams and embedded longitudinal bars. These overstrengths will be significantly higher than those employed in typical capacity design using A23.3–19 recommendations.

- The effect of embedded longitudinal bars should not be neglected in calculating the overstrength in specimens with this characteristic. The median overstrength of specimens without axial restraint and without embedded longitudinal bars is equal to 1.25. This ratio is equal to 1.25 and 1.3 for ELB and AR + ELB, respectively.
- The median amount of overstrength in which the effect of embedded longitudinal bars is considered to be around 1.75 for specimens with slab. This value was equal to 1.4 and roughly 1.5 for specimens that were restrained in an axial direction with PT rods and rigid walls, respectively.
- The median value of ($\theta_{80\%}$) for specimens with PT rods or slabs is almost the same and equal to 8%. This value equals 7% for specimens without any axial restraint. In the specimens with rigid axial restraint, the median value of $\theta_{80\%}$ is equal to 4.9%.
- Full beam confinement is an effective approach that could be implemented for diagonally reinforced coupling beams. It has been observed that by using this type of confinement, the inelastic rotation capacity $\theta_{80\%}$ can meet the existing A23.3 requirements and, in some cases, will outperform the diagonal confinement approach.
- $\theta_{80\%}$ would increase by incrementing transverse reinforcement ratio (ρ_v) in specimens with full beam confinement layout. However, in specimens with diagonal confinement layouts, the enhancement of ρ_v would not significantly impact the value of $\theta_{80\%}$.
- The suggested modification factors for decreasing the shear area and gross moment of inertia of coupling beams by CSA A23.3–19 ($\alpha_s = 0.45$ and $\alpha_f = 0.25$) results in a high initial stiffness which could be considered an upper bound of the studied specimens. We found that $\alpha_s = 0.1$ and $\alpha_f = 0.25$ are reasonable estimates based on the studied specimens.

Acknowledgements This study has been made possible due to the data from many researchers who have completed experimental testing on diagonally reinforced coupling beams. We are thankful to all of these researchers, particularly those who shared their experimental data.

References

1. Paulay T, Binney JR (1974) Diagonally reinforced coupling beams of shear walls. Special Publ 42:579–598
2. Barney GB, Shiu KN, Rabbit BG, Fiorato AE, Russell HG, Corley WG (1980) Behavior of coupling beams under load reversals (RD068.01B). Portland Cement Association, Skokie, IL
3. Ishikawa Y, Kimura H (1996) Experimental study on seismic behavior of R/C diagonally reinforced short beams. In: Proceedings of the 11th World Conference on Earthquake Engineering, Paper (No. 1386)

4. Sonobe Y, Kanakubo T, Fujisawa M, Tanigaki M, Ökamoto T (1995) 41 Structural performance of concrete beams reinforced with diagonal frp bars
5. Galano L, Vignoli A (2000) Seismic behavior of short coupling beams with different reinforcement layouts. ACI Struct J 97:876–885
6. Gonzalez E (2001) Seismic response of diagonally reinforced slender coupling beams (Doctoral dissertation, University of British Columbia)
7. Dugas DG (2002) Seismic response of diagonally reinforced coupling beams with headed bars
8. Kwan AKH, Zhao ZZ (2002) Cyclic behaviour of deep reinforced concrete coupling beams. Proc Inst Civil Eng-Struct Build 152(3):283–293
9. Zhou J (2003) Effect of Inclined reinforcement on the seismic response of coupling beams, M. Eng. Thesis, McGill University. Montreal
10. Shimazaki K (2004) De-bonded diagonally reinforced beam for good repairability. In: 13th World conference on earthquake engineering, Paper (vol 3173)
11. Canbolat BA, Parra-Montesinos GJ, Wight JK (2005) Experimental study on seismic behavior of high-performance fiber-reinforced cement composite coupling beams. ACI Struct J 102(1):159
12. Yun HD, Kim SW, Jeon E, Park WS, Lee YT (2008) Effects of fibre-reinforced cement composites' ductility on the seismic performance of short coupling beams. Mag. Concrete Res. 60(3):223–233
13. Fortney PJ, Rassati GA, Shahrooz BM (2008) Investigation on effect of transverse reinforcement on performance of diagonally reinforced coupling beams. ACI Struct J 105(6):781
14. Naish D, Fry A, Klemencic R, Wallace J (2013) Reinforced concrete coupling beams-part I: testing. ACI Struct J 110(6):1057
15. Lim E, Hwang SJ, Wang TW, Chang YH (2015) An Investigation on the Seismic Behavior of Deep Reinforced Concrete Coupling Beams. ACI Struct J 113. https://doi.org/10.14359/51687939
16. Lim E, Hwang SJ, Cheng CH, Lin PY (2016) Cyclic tests of reinforced concrete coupling beam with intermediate span-depth ratio. ACI Struct J 113(3)
17. Howard B (2017) Seismic response of diagonally reinforced coupling beams with varied hoop spacings. McGill University, Montreal, Canada
18. Poudel A, Lequesne RD, Lepage A (2018) Diagonally reinforced concrete coupling beams: effects of axial restraint. University of Kansas Center for Research, Inc
19. Han SW, Kim S, Kim T (2019) Effect of transverse reinforcement on the seismic behavior of diagonally reinforced concrete coupling beams. Eng Struct 196:109307. https://doi.org/10.1016/j.engstruct.2019.109307
20. Ameen S, Lequesne RD, Lepage A (2020) Diagonally reinforced concrete coupling beams with grade 120 (830) High-Strength Steel Bars'. ACI Struct J 117(6)
21. American Concrete Institute (2020) Building code requirements for structural concrete (ACI 318–19): An ACI Standard; commentary on building code requirements for structural concrete (ACI 318R-19)
22. Design of Concrete Structures (2019) Toronto, Ontario: CSA Group
23. National Building Code of Canada, 2015 (2018) Ottawa, Ont.: National Research Council Canada